INFLUENCE OF ABSOLUTE PRESSURE ON THE COOLING OF A PLATE BY IMPINGING AIR JETS

Robert D. Haberstroh
Robert N. Meroney
In-Kun Kim

College of Engineering
Colorado State University
Fort Collins, Colorado 80521

September, 1970

CER70-71RDH-RNM-IK26

INFLUENCE OF ABSOLUTE PRESSURE ON THE COOLING OF A PLATE BY IMPINGING AIR JETS

Robert D. Haberstroh
Robert N. Meroney
In-Kun Kim

College of Engineering
Colorado State University
Fort Collins, Colorado 80521

September, 1970

CER70-71RDH-RNM-IK26

ABSTRACT

An experimental investigation to determine the effect of absolute pressure on the convective heat transfer coefficient for a hot plate cooled by impingement of air jets upon it was executed as proposed by Haberstroh and Meroney.[1] Variation of absolute pressure was simulated by changing the pressure of a box in which the present experiments are made. Experiments are made at several values of absolute pressure, from 12.3 to 18.3 psia.

Several authors' experimental results obtained under somewhat similar conditions are compared with the present results, and differences are discussed. Data are presented in three ways: the first is the tabulation of raw data; the second shows the relationship between heat transfer coefficient and jet velocity with pressure as a parameter; and the third puts all the data into a single relationship between two dimensionless parameters, Reynolds number and Nusselt number.

After the data from the present experiment are correlated in dimensionless form, the results are applied to prediction of the mass transfer coefficient by way of Reynolds analogy. An illustration of application to design and the ultimate influence of pressure on mass transfer is provided.

INTRODUCTION

There are many indications that the forced-convection heat-transfer process may be sensitive to atmospheric pressure. Specifically, if the heat-transfer fluid is a gas such as air, the density (and thus the kinematic viscosity) varies almost linearly with absolute pressure. Since the kinematic viscosity enters the Reynolds number, the principal independent parameter of forced convection, in the denominator, one would be led to believe that a reduction in absolute pressure would reduce heat transfer, all other factors being unchanged.

As such a reduction could be important to the design or operation of heat-transfer equipment moved from low altitude to high altitude, experiments were undertaken to provide direct confirmation of the expected influence of pressure on heat transfer. The specific forced-convection device in question is a parallel-plate drier in which hot, dry air is caused to impinge roughly normally on the surface to be dried, the air being supplied through a perforated plate. The level of investment in large equipment depending upon this process is such as to justify a direct test of performance *versus* altitude. Although various authors (referred to later) correlate their heat-transfer data against one Reynolds number or another, thus implying the intuitively suspected dependence on pressure, none of the previous investigators reports having varied the pressure to vary the Reynolds number. It is more convenient to alter the Reynolds number by changing the flow velocity. This study undertakes to confirm that the heat-transfer performance of the perforated-plate drier is controlled by the Reynolds number and that the effect is the same if the Reynolds number is changed by changing the pressure or the velocity or both.

EXPERIMENTAL MODEL

The direct experiments calls for a "variable-density wind tunnel" created especially for the purpose. In the present situation an open-cycle tunnel would have made an air cooler unnecessary, but the power requirement of such a tunnel would exceed the capacity of the available fan. Thus a closed-cycle tunnel with cooling of the return air was indicated. This device, illustrated in Figure 1, is described in the sections which follow.

TEST CHAMBER

A wooden box of dimensions 4' X 5' X 6' was built with a removable door on the front side. Walls are made of two layers of 3/4" plywood reinforced by 2" X 4" and 4" X 4" joists running between them. A frame with 3" X 3" X 1/4" steel angles was built with every corner welded, and the prefabricated walls are bolted with 3/8" bolts at six-inch spacing. Inner sides of the walls were coated with epoxy paint and again sealed with building sealant very carefully. The space between the plywood layers is filled with glass wool for sound insulation. With the door bolted on, the resulting wooden pressure vessel is capable of sealing an internal pressure of about 10 psig, at which value the leakage flow is equal to the available flow of pressurizing air.

The elevated pressure in the test tank is maintained by the laboratory air supply. The inlet air is dried by a dessicant, and its pressure is appropriately regulated. The tank pressure is measured by a precision gauge which was recalibrated especially for the present experiment.

The tank is divided by partitions into a high-pressure plenum chamber and a low-pressure return duct. The pressure difference and test-section mass flow are maintained by a 5-HP centrifugal fan whose output is sufficient to give a jet velocity over 200 fps through the test-section perforations. The energy added to the circulating air by friction and test-section heating is removed by a water-cooled heat exchanger; the cooler permits steady-state operation of the equipment. The circulating flow is caused to pass through the heat-transfer test section, which is described next.

TEST SECTION

The test section is a flow passage bounded on the top by a perforated air-supply plate, on the bottom by the surface of the heater, and on three sides by insulated walls which separate the two plates by a distance of 3/4". The fourth side is open to allow departure of the hot air.

Two perforated air-supply plates are used in the present experiment. The first, referred to as plate number 1, has 42 .180"-diameter holes whose ratio of free-flow area to gross plate area (perforation ratio) is 0.743%. This plate is used most widely in the experiments. The second plate (number 2) is used less extensively; it contains 63 .180" holes at 1.112% perforation ratio.

The test surface is a polished aluminum plate of lateral dimensions 1' X 1' and thickness of 1/2". Four strip heaters of 1 Kw capacity each are attached with bolts under the aluminum plate in such a way that the temperature distribution in the plate can be arbitrarily controlled by variacs installed on a control panel outside the box. Inputs to each heater are calculated from the resistance of the heater and the applied voltage which is read from an AC voltmeter on the control panel. Glass wool insulation 4" thick is placed under the heating strip to reduce conduction loss out the bottom to less than 1% of the input to the heating strips.

Thermocouples are mounted in grooves under the aluminum plate at a distance of 1/100" from the surface. A total of eleven thermocouples are installed in the test section, eight of them mounted on the plate, one in the guard heater, one in the plenum chamber, and one at the test-section exit. All of the temperatures are read by a digital thermocouple thermometer.

Air mass flow and velocity are measured by use of the first law of thermodynamics

$$q = \dot{m} C_p (T_a - T_e) \quad , \tag{1}$$

where T_a is the hot-air supply temperature and T_e is the air temperature at the exit of the test section. As all the quantities in (1) are known except $\dot{m}$, this equation gives a precise and convenient measure of mass flow. The density is taken at the average of plenum and plate temperatures, and the continuity equation then gives the velocity. An ASME square-edge orifice was included in the 4" air circulation pipe, but it was found that leakage between the high- and low-pressure sides of the chamber was enough to make very significant errors in the mass flow as measured by this orifice, except at atmospheric pressure where the orifice measurement confirmed the calculation from Eq. (1).

TEST CONDITIONS AND PROCEDURES

The test conditions are slightly changed from the previously proposed ones partly due to the reduced free flow area of the perforated plate and partly due to the experimental results which differed slightly from those expected.

Jet velocities are from 25 fps to 200 fps instead of 0 to 100 fps, because the lower the velocity, the higher the possibility of making an error in the calculation of velocity. The plate temperatures are between 140 and 260°F. Maximum absolute pressure is reduced to 18.3 psia instead of 25 psia.

With the pressure set and the input voltage adjusted to give uniform temperature on the plate, air is circulated giving appropriate impinging velocity on the heating plate. The temperatures of the eleven thermocouples are recorded at the proper time intervals to determine when steady state is reached. When a steady state is established for both plate and plenum-chamber temperatures, a heat-transfer coefficient is calculated and the next experiment is executed for different velocities. When the experiment at one input voltage covers the velocity range, input voltages are changed and an experiment at a different temperature value is undertaken.

RESULTS

The raw data for temperature, velocity, heat transfer, and convection heat-transfer coefficient defined as

$$h = \frac{q/A}{T_{plenum} - T_{plate}} \tag{2}$$

are listed for the two plates in Table I. These data are plotted in terms of h vs. V_o in Figures 2 and 3, one for each of the perforated plates tested. In these curves the parameter is ambient pressure, and it is seen that all the curves are parallel; they all follow the same power law. (Properties are evaluated at a film temperature which is the linear average of the plenum temperature and the plate temperature.)

Plotting the Nusselt number

$$\mathrm{Nu} = \frac{hD_o}{k}$$ against a Reynolds number defined as

$$\mathrm{Re} = \frac{V_o D_o}{\nu}$$

brings all the data together onto a single curve as in Figures 4 and 5. Thus the suspected influence of the Reynolds number is confirmed, and a direct test of the significance of the density in the Nu vs. Re relation has been executed. Empirical equations which describe these data are

$$\mathrm{Nu} = .00453\,\mathrm{Re}^{.98} \tag{3}$$

(1500 < Re < 14,000) for plate number 1,

and

$$\mathrm{Nu} = .0230\ \mathrm{Re}^{.82} \tag{4}$$

(2500 < Re < 13,000) for plate Number 2.

These lines are plotted through the data in Figures 4 and 5.

COMPARISON WITH OTHER INVESTIGATIONS

The large number of possible independent variables (flow rate, pressure, hole spacing, hole diameter, and plate spacing) in perforated-plate heat-transfer equipment, coupled with the fact that most prior investigations have had specific design applications in mind, tends to make direct comparison with other data difficult or inconvenient. Further, although it is well known that industrial firms have conducted tests of their own equipment for design purposes, the tendency is for the equipment makers to avoid publication of the results; there are no doubt very many useful data in existence with which no comparison is possible for this reason. Even so there are a few references which permit at least general discussion in the context of the present experiment.

The principal works of interest, referred to in a General Electric Co. "Design Data" report are those of Kercher[2] and Hilgeroth[3]. These results are useful for comparison mainly because the hole patterns are generally similar to the present ones, some accounting is made of the orifice geometry, and mention is made of the means of conducting away the exit flow. Further, these two investigators correlated their results in terms of Reynolds and Nusselt numbers which are susceptible to interpretation in the terms used in the present study.

The most direct comparison is that with Kercher's[2] equation

$$\frac{hD_o}{k} = \phi_1\phi_2\left(\frac{vD_o}{\nu}\right)^m\left(\frac{Zn}{D_o}\right)^{.091}\left(Pr_o\right)^{1/3} \qquad (5)$$

in which the coefficient ϕ_1 and the exponent m are influenced by the hole spacing and the Reynolds number itself. ϕ_2 is a coefficient to account for the "spent flow effect" which reduces the average heat-transfer coefficient by deflecting the impinging jets of air. Kercher provides curves for these parameters, and if appropriate values are inserted for the present test conditions, the results are as shown in Figures 4 and 5. It is seen that Kercher's results show about the same power-law dependence as the present ones, but Kercher's coefficient is about 20% lower than the present one. A possible reason for a difference, though not necessarily for the <u>direction</u> of the difference, lies in the fact that Kercher's holes were arranged in a regular, square pattern, while the present ones are on a triangular pitch.

The correlation of Hilgeroth[3] is somewhat simpler than Kercher's, but it does not account for the spent-flow effect, except that the log-mean value of the test-section air temperature minus the plate temperature is used in the definition of h. The exponent on the Reynolds number is nearly constant, between 0.72 and 0.78, and this value is noticeably lower than that obtained in either of the two present tests.

Data presented by Freidman and Mueller[5], Lyman[6], and Allander[7] are displayed as direct relations between h and the flow velocity; the implication of a Reynolds number is present, but these investigators, concentrating on other features of flow and design, do not attempt to make generalized correlations. The exponents on velocity, however, range from .64 to .78.

Another correlation, based on extensive data, is furnished by Gardon and Cobonpue[4] for flow from nozzles onto a flat plate. The spacing ratio, important in orifice-to-plate heat transfer, is much larger in the experiment of reference (4) because of the protusion of the nozzles from their base plate. The exponent on Reynolds number is .625, the smallest of all the correlations.

In general all of these presentations, including the present one, predict h vs. V_o within a broad band which varies about ± 33% around the central value. This is perhaps to be expected what with the broad spectrum of geometries and test conditions considered by the various authors.

EXTENSION TO CALCULATION OF MASS TRANSFER COEFFICIENT

In order to assess the influence of pressure on drying, it is necessary to estimate its influence on the mass-transfer coefficient. This extension is based on the well known Reynolds analogy, which has had successful application in many turbulent, unseparated flows. The most common applications have been between heat transfer and momentum transfer, but there have been numerous uses (8, 9, 10, 11) of the analogy between heat transfer and mass transfer.

Considering first Plate number 1, one recalls the empirical equation

$$\mathbb{N}u = .00453\, \mathbb{R}e^{.98}, \qquad (3)$$

which requires some modification to include the effect of Prandtl number. Heat transfer experiments over a wide range of configurations include the Prandtl number to the 0.4 power, and if this is done, using $\mathbb{P}r \doteq .72$, these results

$$\mathbb{N}u = .00517\, \mathbb{R}e^{.98}\, \mathbb{P}r^{.4} \qquad (6)$$

In the Reynolds analogy transformation the Nusselt number goes to the

Sherwood number, the Reynolds number remains the same, and the Prandtl number goes to the Schmidt number. Thus

$$Sh = .00517\, Re^{.98}\, Sc^{.4} \tag{7}$$

where the Sherwood number $Sh \equiv \frac{h_d D_o}{D_m}$.

Schmidt number $Sh \equiv \frac{\nu}{D_m}$

mass transfer coefficient $h_d \equiv \frac{\text{vapor mass flux.}}{\text{Concentration drop}}$

and D_m is the molecular mass diffusivity.

For calculation the mass transfer coefficient, (7) may be rewritten as

$$h_d = .00517 \frac{D_m}{D_o} \left(\frac{V_o D_o}{\nu}\right)^{.98} (Sc)^{.4} \quad . \tag{8}$$

Now the mass diffusivity and kinematic viscosity both go as $1/\rho$, so the Schmidt number will not vary with pressure. But the D_m and ν in the Sherwood number and in the denominator of the Reynolds number could influence the result. The fact that the exponent on Reynolds number is so very nearly unity causes these two quantities nearly to cancel each other, and for this particular geometry there is for practical purposes no influence of pressure on the mass transfer coefficient. This cancellation does not occur for the heat transfer coefficient, and Eq. (3) shows that h diminishes almost linearly as the pressure decreases.

The second plate, whose heat transfer coefficient follows Eq. (4), shows a predicted mass transfer coefficient of

$$h_d = .0262 \frac{D_m}{D_o} \left(\frac{V_o D_o}{\nu}\right)^{.82} (Sc)^{.4} \quad . \tag{9}$$

The exponent on the Reynolds number is smaller, and the influence of D_m against $\nu^{-.82}$ gives a weak increase of h_D with decreasing ambient pressure. As will be shown in the next section, however, there are other considerations which will overshadow this effect.

APPLICATION TO DESIGN

In order to see the influence of absolute pressure on the high-altitude performance of a drier, it is necessary to go beyond merely calculating the heat and mass transfer coefficients. As will be evident in the discussion which follows, the ambient pressure enters the calculation in several ways, and it is necessary to execute the complete computation of the vapor flow in order to see the full effect of pressure changes. Accordingly a simple model of a drier is presented here. Except in the details of the relationship between the heat and mass transfer coefficients (h and h_d) and the flow of drying air ($\dot{m}_a$), this could be a model of any dryer. The point is to assess the role of atmospheric pressure on the combined heat-and-mass-transfer problem which arises when dry air blows over a plate whose surface is continuously wet with liquid water.

The first law of thermodynamics for the liquid film states that the removal of latent heat by the outflow of vaporized water must be supplied by the convective heat transfer from the hot, dry air to the liquid surface. Thus

$$\dot{m}_v H_{fg} = hA(T_a - T_s) , \qquad (10)$$

where T_a is the temperature of the dry air, T_s is the temperature of the liquid film, and A is the surface area for transport. The problem is to find $(\dot{m}_v/A)$. Since T_s is a function of T_a and other independent variables, it must be found or eliminated as a dependent variable.

The rate of mass transfer may also be computed from the definition of the mass transfer coefficient; thus $\dot{m}_v = h_d A(C_s - 0)$, where C_s is the concentration of water vapor at the surface of the film, and the concentration in the drying air is taken as zero. It is convenient to rewrite the surface concentration of water vapor in air in terms of the saturation partial pressure P_{v_s}; thus

$$\dot{m}_v = \frac{h_d A}{R_v T_s} P_{v_s} \quad , \tag{11}$$

where R_v is the gas constant for water vapor.

Now P_{v_s} remains as an unknown, but it is convenient to manipulate the Clapeyron equation to give P_{v_s} in terms of T_s. If one makes the common assumptions of $v_g >> v_f$ and a perfect-gas relation for the water vapor, one can integrate the Clapeyron equation from some base value of pressure P_o and temperature T_o to give

$$P = P_o \exp \frac{H_{fg}}{RT} (\frac{T}{T_o} - 1) \quad , \tag{12'}$$

and if steam-table values at T_o = 100F (arbitrarily chosen) are used, one obtains

$$P_{v_s} = 136.3 \exp 16.81 \left(1 - \frac{560}{T_s}\right) \tag{12}$$

where P_{v_s} is in psf. This relation has been tested by the authors over the range $40 < T_s < 160$F; it shows errors of about ± 1% as compared with steam-table data. The closed form of (12) will simplify the continuing analysis.

The system of Equations (10), (11), and (12) is then to be solved for $\dot{m}_v$, T_s and P_{v_s}. The independent variables are for the moment h, h_d (both known by the correlation and Reynolds' analogy), and T_a. The first step toward solution is to put (12) into (11) and to eliminate $\dot{m}_v$ between the result and (10). There follows

$$e^{-16.81(1 - \frac{560}{T_s})} T_s(T_a - T_s) = 136.3 \frac{H_{fg}}{R_v} \frac{h_d}{h} . \qquad (13)$$

With R_v a constant and H_{fg} roughly constant, one sees that the film temperature depends only on T_a and the ratio of the two transport coefficients. In fact if the two correlations (6) and (7) are used to give the ratio of the h's, there results

$$\frac{h_d}{h} = \frac{D_m}{k} \frac{\mathbb{S}c^{.4}}{\mathbb{P}r} = \frac{1}{\rho c} \mathbb{L}e^{-.6}$$, in which the Lewis number is defined as

$$\mathbb{L}e = \frac{\mathbb{S}c}{\mathbb{P}r} = \frac{\alpha}{D_m} ,$$

where α is the thermal diffusivity and D_m is the mass diffusivity. The interesting outcome, if this result is put into Eq. (13), is that under the Reynolds analogy assumption the saturation film temperature in the steady state is independent of the air mass flow and in general of the fluid mechanics. Eq. (13) is rewritten in these terms as

$$T_s(T_a - T_s)\, e^{-16.81(1 - \frac{560}{T_s})} = 136.3 \frac{H_{fg}}{R_v} \frac{1}{\rho c} \mathbb{L}e^{-.6} \qquad (13)$$

The only place where the absolute pressure can enter is in the ρ on the right-hand side, and if the temperature is taken to be roughtly T_a and the density roughly that of dry air, then one obtains

$$\rho = \frac{144}{53.3} \frac{P}{T_a} = 2.70 \frac{P}{T_a} \quad \text{(P in psia)}$$

which is to be put into Eq. (13). The result is transcendental in T_s, but it is conveniently soluble graphically for T_s vs. P with T_a as a parameter. T_s is quite nearly linear with P over the range $10 < P < 20$ psia and $100 < T_a < 250F$, and this linearity may be used for convenient manipulation leading to the desired mass flow of vapor.

It appears that Equation (10) is the convenient source of $\dot{m}_v$ in the form

$$\frac{\dot{m}_v}{A} = \frac{h(T_a - T_s)}{H_{fg}} \tag{10}$$

As the needed form of T_s is $(T_a - T_s)$, one plots the difference and finds it to be very nearly linear with both pressure and hot-air temperature over the ranges in questions. The result for this particular case is

$$(T_a - T_s) = .862\, T_a - 25.2 - (.68 + .00573\, T_a)\, P \quad , \tag{14}$$

where P is in psia and the temperatures are in Fahrenheit.

The heat transfer convection coefficient h is obtained from correlations such as (3) and (4). Up to the present the specific geometry and fluid mechanics of the apparatus have not entered the analysis, but inclusion of a correlation for h immediately ties the calculation to a particular style of drier. For simplicity in computation, the Reynolds number exponent of Eq. (3) will be taken as 1.0 instead of the more accurate 0.98. The error is not great compared with other approximations already incorporated. Then

$$h \doteq \frac{k}{D_o}(.00453)\left(\frac{V_o D_o}{\nu_o}\right) = .00453\,\frac{k}{\mu}\,\rho V_o \quad ,$$

where the unity exponent curiously enough causes the effect of hole size D_o to cancel. In this expression ρ is evaluated at the test section temperature and pressure, and these are reasonably well approximated by T_a and ρ. Then the perfect-gas law gives

$$\rho = \frac{p}{RT_a} = \frac{(144)p}{(53.3)T_a} = 2.70\,\frac{p}{T_a} \quad ,$$

in which the pressure is in psia.

If all these statements are inserted into Eq. (10), the result is

$$\frac{\dot{m}_v}{A} = .00453\frac{k}{\mu}(2.70)\,\frac{PV_o}{T_a'\,H_{fg}}\quad .862\,T_a - 25.2 - (.68 + .00573\,T_a)P \tag{15}$$

where $\frac{\dot{m}_v}{A}$ is in $\#_m$/sec ft^2

$k \doteq .017$ Btu/ft hr°F

$\mu \doteq .047\ \#_m$/ft hr

P is in psia

T_a is air temperature in Fahrenheit

T_a' is air temperature in Rankine (same quantity)

$H_{fg} = 1037.2$ Btu/$\#_m$, chosen at 100 F

and V_o is in ft/sec

If these numbers are inserted, the final estimate of $\dot{m}_v/A$ is

$$\frac{\dot{m}_v}{A} = 4.27\cdot 10^{-6}\ \frac{PV_o}{T'_a}\left\{.862\ T_a - 25.2 - (.68 + .00573\ T_a)P\right\} \tag{15}$$

$$100 < T_a < 250\ F\ ,\qquad 10 < p < 20\ \text{psia.}$$

Eq. (15) is plotted against the absolute pressure in Figure 6. The influence of the dry air temperature and flow velocity are visible in the parametric curves. The air temperature's major effect is in raising the film temperature and thus the saturation partial pressure. There is a less important negative effect which arises from the reduced ΔT for heat transfer as T_s increases. The air velocity influences the performance in a routine multiplicative way; it appears as a linear multiplier because of the earlier simplification of the exponent on the Reynolds number.

The ambient pressure appears in two ways. The first is in the leading term, which is the density contribution to the convective heat-transfer coefficient. This is the more important of the two effects, as indicated by the nearly linear increase of $\dot{m}_v/A$ with p in Figure 6. The second effect of pressure is a slightly reducing effect which again arises from the increase of T_s with p. Increased T_s gives reduced $(T_a - T_s)$, _ceteris paribus_, and thus a reduced ΔT for heat transfer.

It is evident from Figure 6 that in an ordinary range of the independent variables the mass flux increases with increasing ambient pressure. It is instructive to estimate from this result the deterioration of mass flux which might occur in moving a piece of drying equipment from sea level (14.7 psia) to the elevation of Fort Collins, 5000 feet (12.5 psia). Over the range plotted, Figure 6 shows reductions from 11% to 13.7%, the higher figure being for the highest temperatures and velocities. These values may be compared with the 15% reduction of atmospheric pressure.

CONCLUSIONS

The conclusions may be summarized as follows:

1. The effect of ambient pressure on the heat transfer coefficient enters by the effect on kinematic viscosity in the denominator of the Reynolds number. As pressure increases, heat transfer coefficient increases according, for example, to Eq. (3).
2. The effect of pressure on mass transfer coefficient is weak, according to a Reynolds analogy prediction, Eq. (8).
3. The entire heat- and mass-transfer situation must be considered to provide a proper estimate of the effect of pressure. It is necessary to solve Eq's. (10), (11), and (12) to obtain the effect of ambient pressure on the water-vapor mass flux.
4. As a general rule, and especially in the practical range of air-impingement dryer design, a reduction in atmospheric pressure causes a reduction in water-vapor mass flux, all other things being equal.

1. Haberstroh, R. D. and Meroney, R. N., A proposal to Eastman Kodak Company for an Experimental Project, "Absolute Pressure Effect in Impingement Dryers," November 1969.

2. Kercher, D. M., "Heat Transfer by a Multiple Array of Round Air Jets Impinging Perpendicular to a Flat Surface Including Effect of Spent Air," General Electric Company TIS Report R67FPD 299, 1967.

3. Hilgeroth, E., "Heat Transfer for Jet Flow Perpendicular to the Exchange Surface," General Electric Translation Folder 6883.

4. Gardon, R. and Cobonpue, J., "Heat Transfer Between a Flat Plate and Jets of Air Impinging on It," 1966 International Heat Transfer Conference, August 28-September 1.

5. Freidman, S. J. and Mueller, A. C., "Heat Transfer to Flat Surface," Proc. General Discussion on Heat Transfer, Institution of Mechanical Engineers, London, 1951, pp. 138-142.

6. Lyman, L. C., "Effect of Air Flow on Heat Transfer and Water Evaporation in Jet Drying Systems," Forest Product Journal, October 1965, pp. 453-458.

7. Allander, C., "Air Impingement Drying," Tappi, Vol. 44, No. 5, May 1961, pp. 332-337.

8. Bird, R. B., Stewart, W. E., and Lightfoot, E. N., Transport Phenomena, New York, John Wiley & Sons, Inc., 1960.

9. Eckert, E. R. G., and Drake, R. M., Jr., Heat and Mass Transfer, New York, McGraw-Hill Book Company, Inc., 1959.

10. Rohsenow, W. M., and Choi, H. Y., Heat, Mass, and Momentum Transfer, Englewood Cliffs, N. J., Prentice-Hall, Inc., 1961.

TABLE I

RAW DATA FOR PLATE NUMBER ONE

P = 12.3 psia

T_p(F)	T_∞(F)	V_o(ft/sec)	h(Btu/hrft^2°F)	q(Btu/hr)
172.3	109.6	134.0	33.8	2120
165.0	105.0	191.0	44.9	2690
165.2	107.4	137.0	37.2	2150
199.0	102.1	102.0	28.7	2210
218.1	119.9	80.6	20.75	2050
183.2	107.8	108.0	28.2	2130
233.5	115.7	86.5	22.1	2606
209.3	113.6	84.7	21.6	2080
168.5	110.1	79.1	21.7	1270
207.3	109.5	121.0	31.6	3130
175.2	103.3	113.5	28.8	2065
153.1	108.2	117.0	29.8	1340
179.6	112.8	153.2	40.8	2690
154.2	111.2	160.0	41.5	1770
131.7	107.8	165.0	43.4	1042
177.7	105.5	121.5	31.9	2300
175.8	109.8	162.0	42.6	2810
160.4	104.9	84.2	22.7	1260
179.5	104.2	135.0	34.3	2590
212.7	110.6	87.4	21.4	2180
157.1	103.2	192.0	48.8	2620
159.9	105.5	170.6	47.6	2590
219.1	112.9	90.9	24.6	2610
231.7	104.1	47.0	10.3	1305
274.9	107.7	26.2	5.92	990
235.8	107.0	30.5	7.87	1015

P = 14.3 psia

T_p(F)	T_∞(F)	V_o(ft/sec)	h(Btu/hrft^2°F)	q(Btu/hr)
182.7	107.8	117.0	35.0	2620
168.3	105.0	155.0	43.6	2690
155.2	106.7	183.0	54.5	2640
224.6	113.4	71.2	21.0	2335
152.9	108.6	164.0	51.6	2286
159.8	109.1	127.5	41.1	2085
187.5	108.5	102.0	32.8	2590
179.5	106.5	115.0	36.1	2630
166.3	105.5	137.3	42.5	2590
194.2	114.2	81.1	27.0	2160
189.6	120.0	85.3	30.4	2120
223.1	120.2	68.7	20.4	2100
218.3	113.8	69.0	20.6	2150
247.8	116.6	64.3	16.85	2210
167.2	113.2	138.7	48.5	2630
164.5	113.5	161.0	49.2	2510
189.7	114.7	93.0	28.3	2120
242.6	115.5	67.3	19.85	2520
221.5	112.8	75.2	23.3	2539
189.9	111.6	94.5	32.7	2570

Table I (cont'd.)

P = 16.3 psia

T_p(F)	T_∞(F)	V_o(ft/sec)	h(Btu/hrft^2°F)	q(Btu/hr)
166.6	111.5	54.0	17.0	2560
216.3	111.2	72.3	25.1	2640
184.8	110.2	98.2	35.0	2615
236.6	117.1	61.0	19.7	2340
187.4	114.0	81.4	30.1	2210
166.0	112.9	106.9	40.9	2180
156.0	110.3	141.5	55.7	2180
235.9	134.4	55.6	21.8	2215
188.7	116.8	82.6	29.5	2180
166.4	109.0	141.1	56.3	3230
185.0	108.2	107.0	41.4	3180
201.1	113.7	93.0	37.0	3260

P = 18.3 psia

156.4	111.6	57.3	23.8	1065
148.7	110.8	70.2	30.5	1160
140.5	109.7	75.8	31.0	956
195.6	109.8	87.5	37.5	3220
176.7	108.7	107.0	47.0	3190
159.3	108.1	136.0	55.1	2820

TABLE 2

RAW DATA FOR PLATE NUMBER TWO

P = 12.3 psia

T_p(F)	T_∞(F)	V_o(ft/sec)	h(Btu/hrft^2°F)	q(Btu/hr)
145.0	95.0	180.5	56.0	2800
149.8	96.1	166.4	51.9	2785
158.4	98.5	144.8	46.5	2790
172.4	99.6	124.6	38.7	2810
179.8	100.7	108.0	35.7	2830
193.3	101.5	88.3	30.5	2810
223.1	100.6	65.3	22.5	2850
165.5	98.4	159.8	49.7	3330
172.5	97.2	144.0	44.1	3310
193.4	100.6	99.8	35.4	3290
213.7	101.9	79.2	29.5	3290
268.4	102.3	58.8	19.8	3300

P = 14.3 psia

154.1	99.2	162.0	60.5	3320
171.6	100.4	132.4	48.0	3415
210.3	98.5	78.3	28.7	3220
163.2	91.5	124.1	46.4	3325
182.5	95.8	106.1	38.0	3290
196.5	94.6	81.5	32.2	3270
269.0	94.5	48.7	18.7	3260

P = 15.3 psia

176.8	90.0	93.9	37.1	3210
202.3	90.1	58.2	24.8	3280
283.1	90.7	39.6	17.3	3330

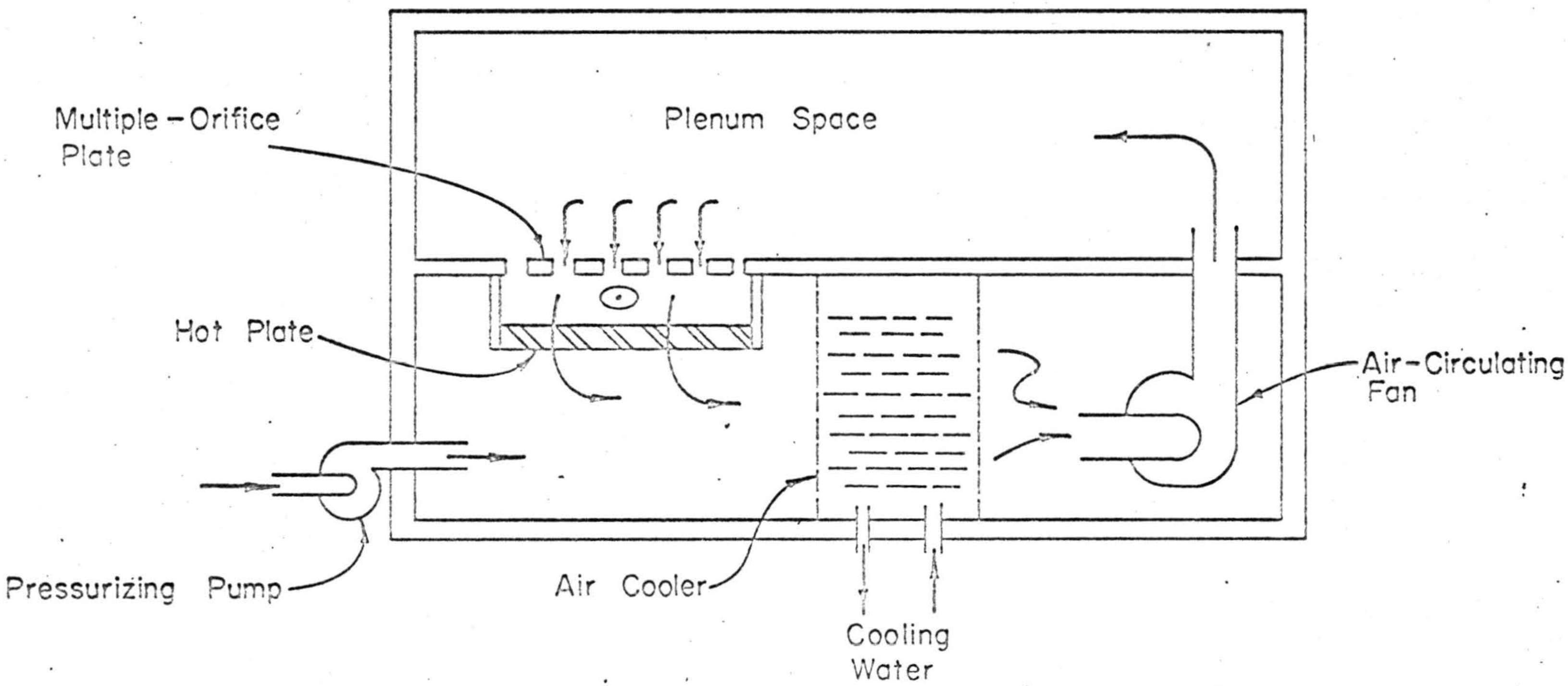

FIGURE 1

SCHEMATIC SKETCH OF FLOW APPARATUS

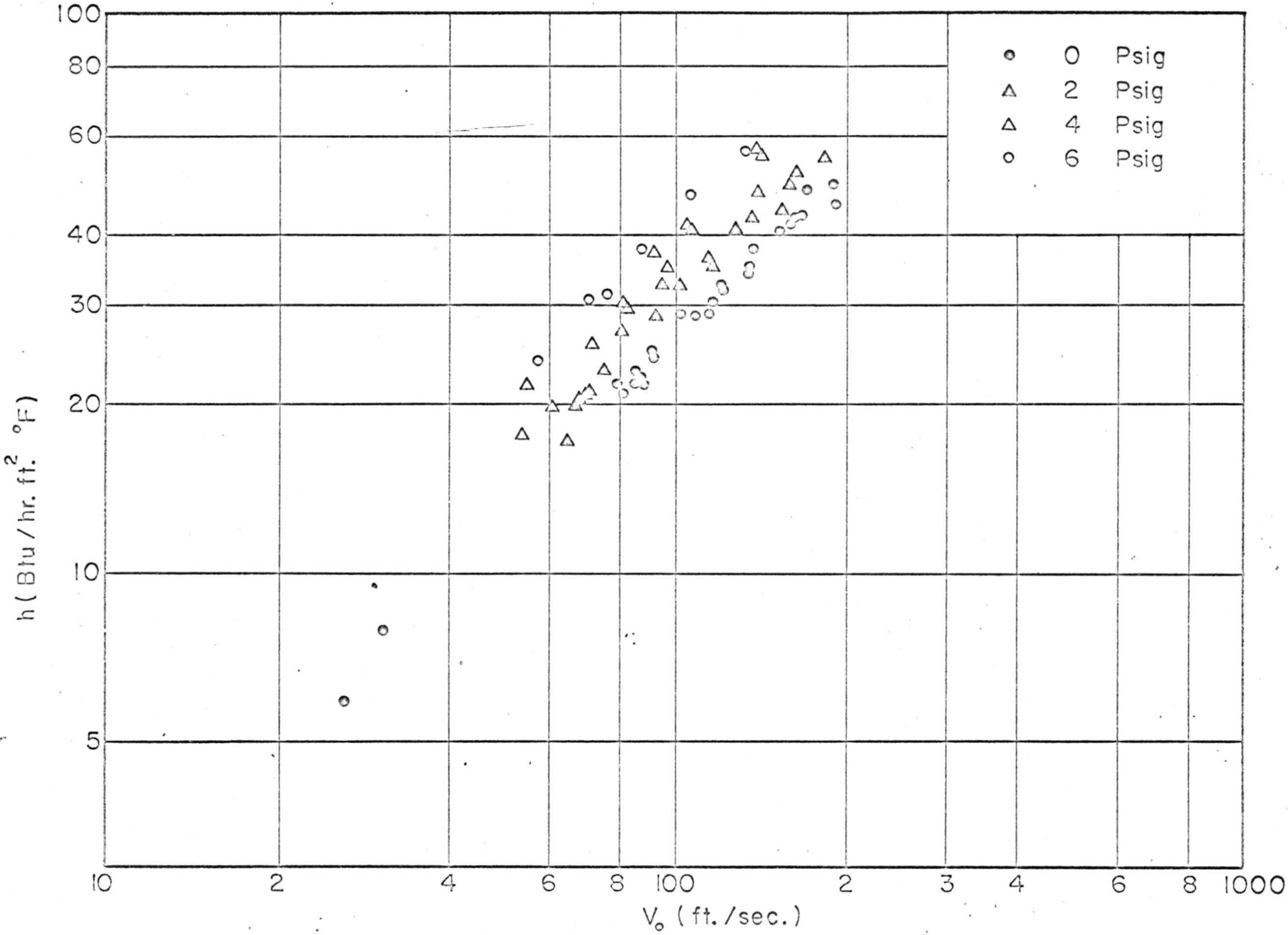
0 Psig
2 Psig
4 Psig
6 Psig
100
80
60
40
30
20
10
5
h (Btu / hr. ft.^{2} °F)
10
2
4
6
8
100
2
3
4
6
8
1000
V_o (ft. / sec.)

Fig. 2

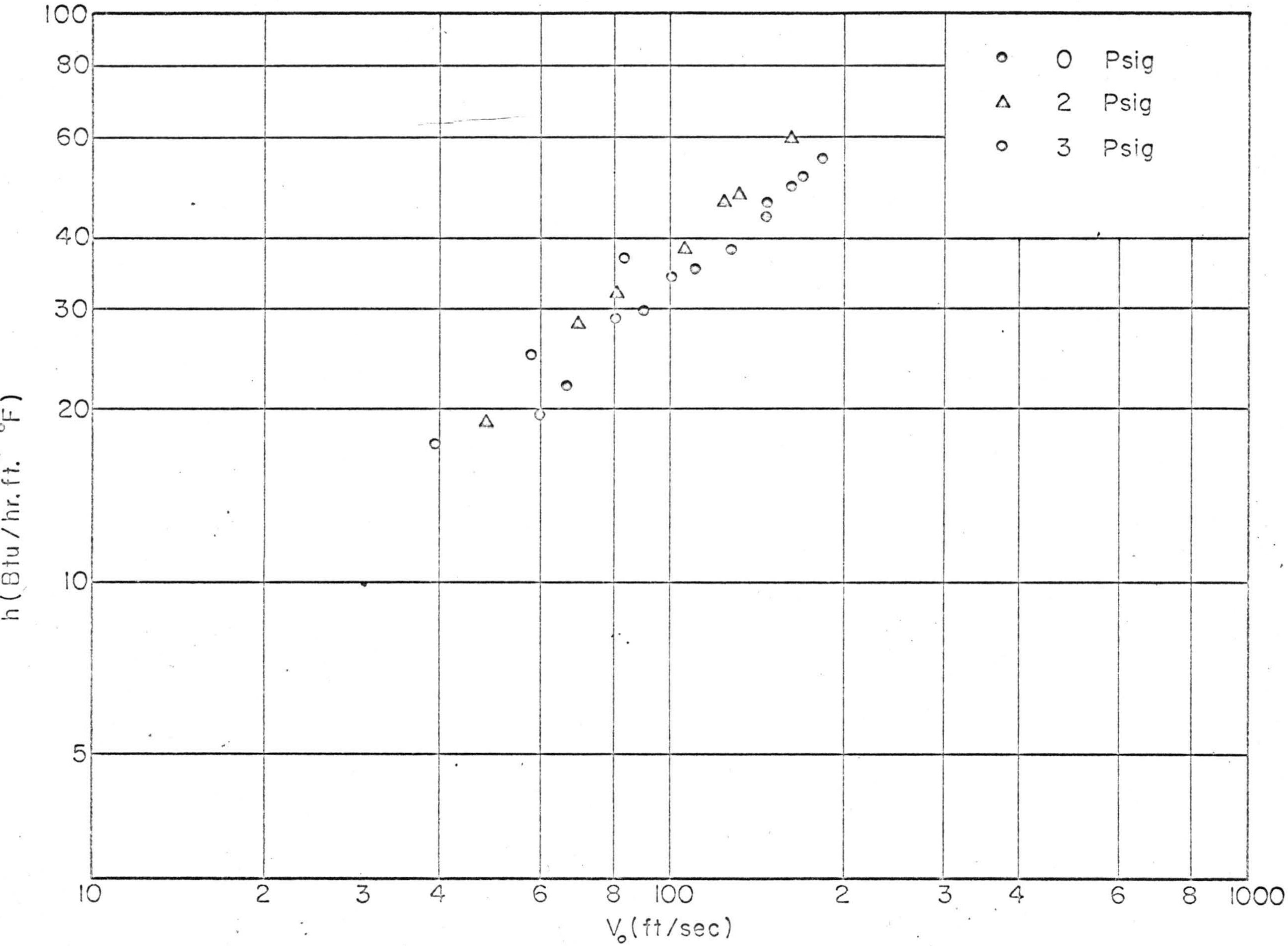

0 Psig
2 Psig
3 Psig
100
80
60
40
30
20
10
5
h(Btu/hr.ft.^{2} °F)
10
2
3
4
6
8
100
2
3
4
6
8
1000
V_o(ft/sec)

Fig. 3

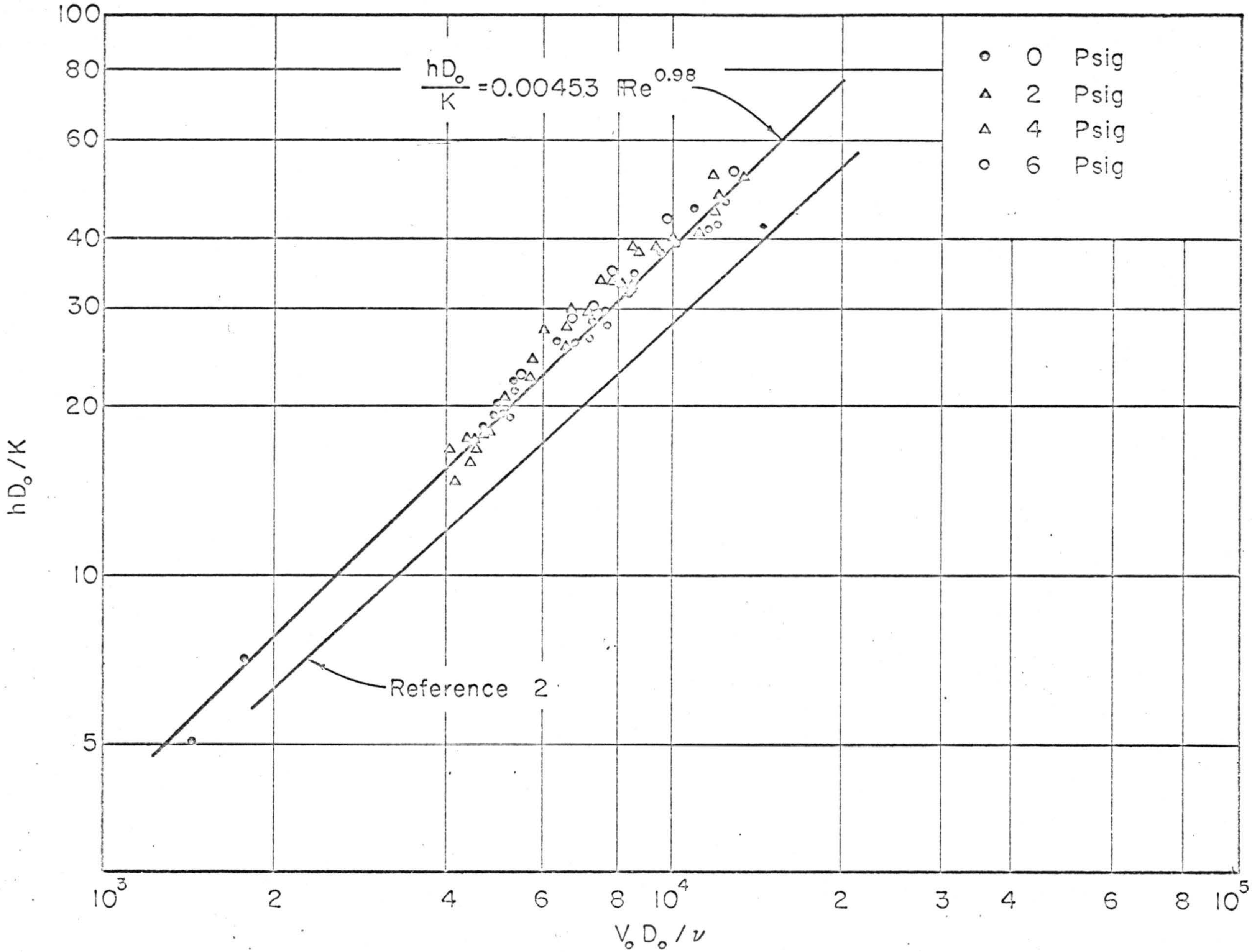
$\frac{hD_o}{K} = 0.00453\ Re^{0.98}$
0 Psig
2 Psig
4 Psig
6 Psig
Reference 2
hD_o/K
$V_o D_o/\nu$
100
80
60
40
30
20
10
5
10^3
2
4
6
8
10^4
2
3
4
6
8
10^5

Fig. 4

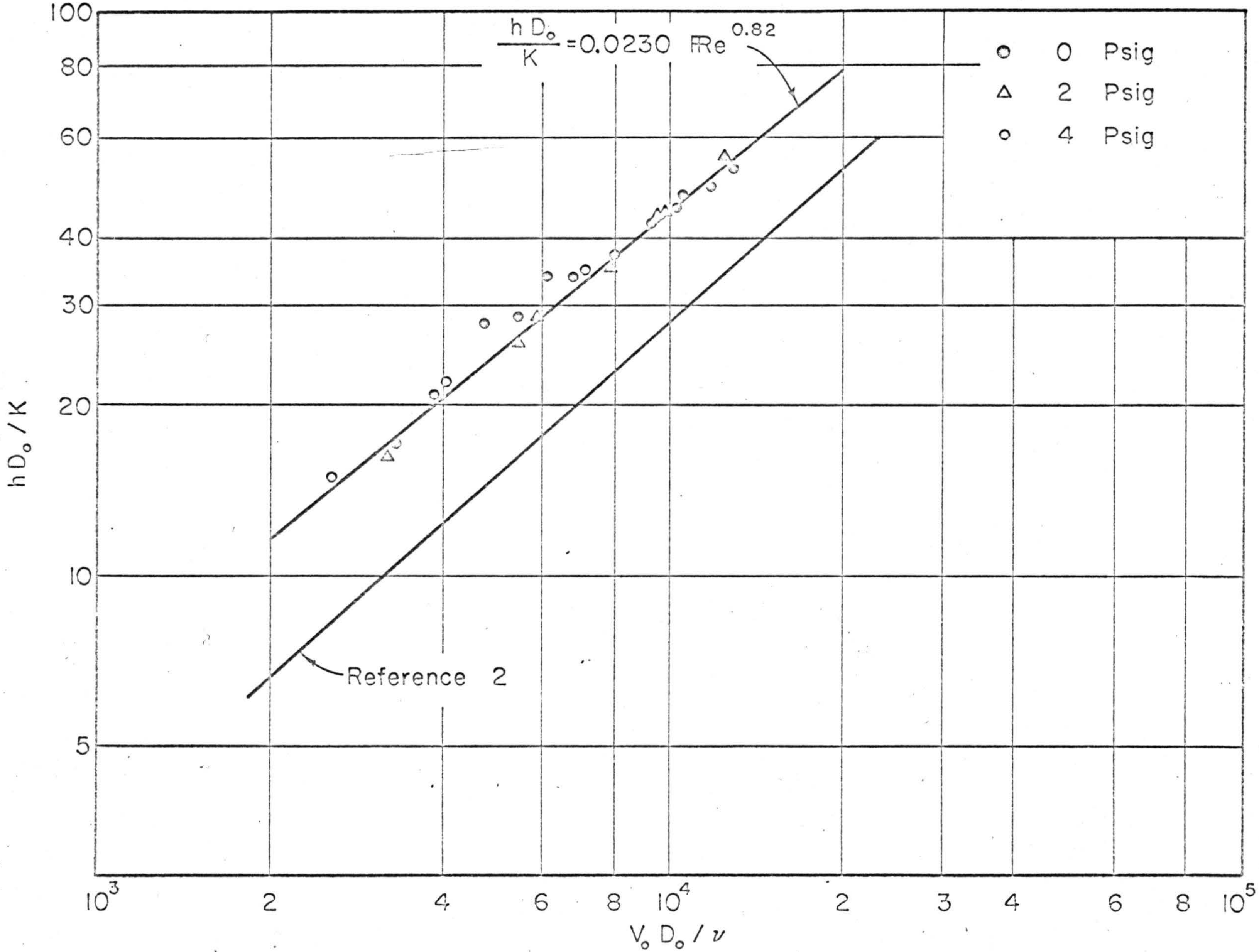

$\frac{hD_o}{K} = 0.0230\ \mathrm{Re}^{0.82}$
○ 0 Psig
△ 2 Psig
○ 4 Psig
Reference 2
hD_o/K
$V_o D_o / \nu$
100
80
60
40
30
20
10
5
10^3
2
4
6
8
10^4
2
3
4
6
8
10^5

Fig. 5

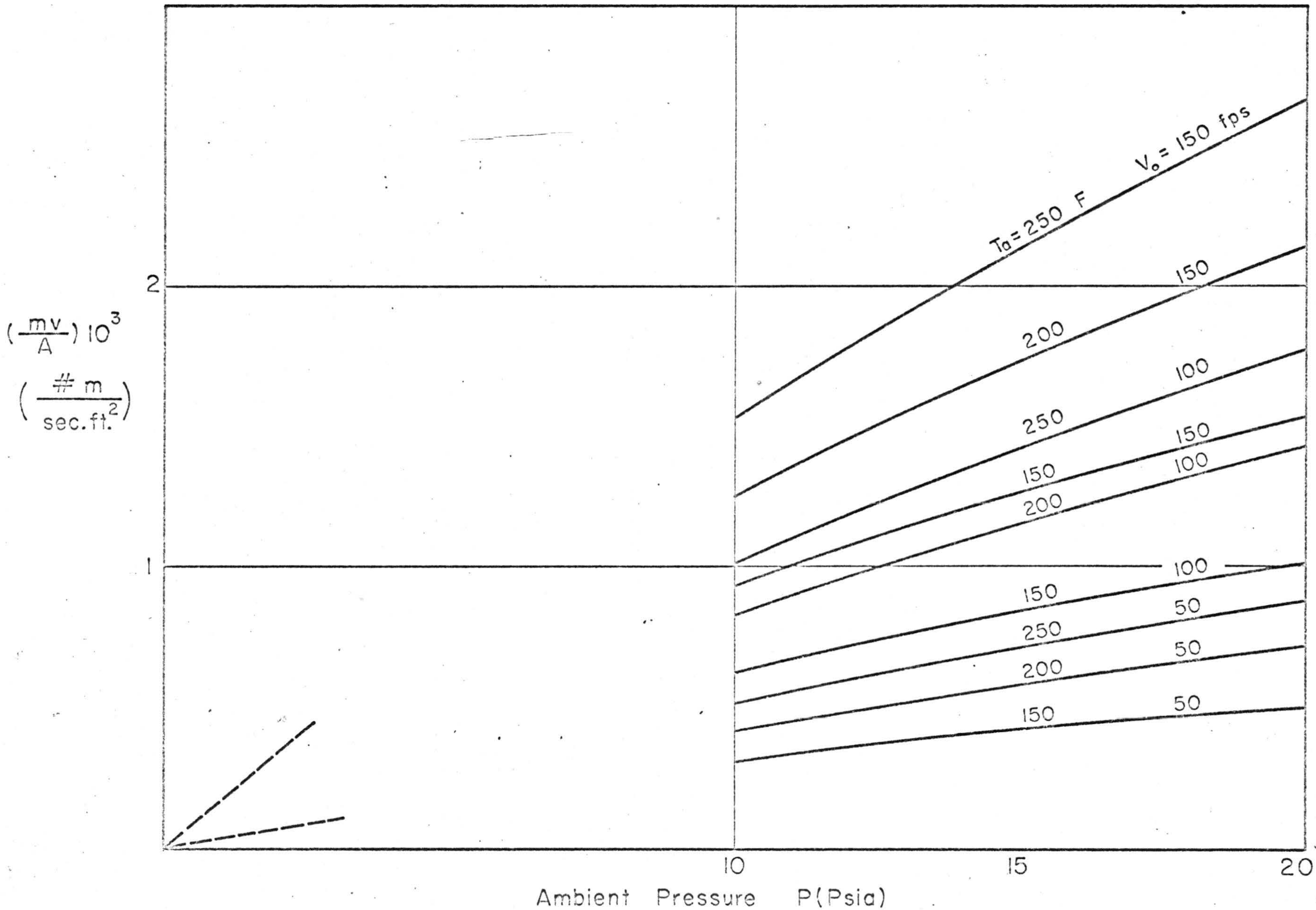
T_a= 250 F
V_o= 150 fps
150
200
100
250
150
100
150
200
100
150
50
250
50
200
50
150
2
1
10
15
20
$(\frac{mv}{A})10^3$
$(\frac{\# m}{sec.ft^2})$
Ambient Pressure P(Psia)

Fig. 6